JACS
JOURNAL OF THE AMERICAN CHEMICAL SOCIETY

Communication

pubs.acs.org/JACS

Near-Infrared-to-Visible Photon Upconversion Sensitized by a Metal Complex with Spin-Forbidden yet Strong S_0–T_1 Absorption

Shogo Amemori,[†,§] Yoichi Sasaki,[†,§] Nobuhiro Yanai,[*,†,‡] and Nobuo Kimizuka[*,†]

[†]Department of Chemistry and Biochemistry, Graduate School of Engineering, Center for Molecular Systems, Kyushu University, 744 Moto-oka, Nishi-ku, Fukuoka 819-0395, Japan

[‡]PRESTO, JST, Honcho 4-1-8, Kawaguchi, Saitama 332-0012, Japan

Supporting Information

ABSTRACT: Near-infrared (NIR)-to-visible (vis) photon upconversion (UC) is useful for various applications; however, it remains challenging in triplet–triplet annihilation-based UC, mainly due to the energy loss during the S_1-to-T_1 intersystem crossing (ISC) of molecular sensitizers. In this work, we circumvent this energy loss by employing a sensitizer with direct S_0-to-T_1 absorption in the NIR region. A mixed solution of an osmium complex having a strong S_0–T_1 absorption and rubrene emitter upconverts NIR light (λ = 938 nm) to visible light (λ = 570 nm). Sensitizer-doped emitter nanoparticles are prepared by re-precipitation and dispersed into an oxygen-barrier polymer. The obtained composite film shows a stable NIR-to-vis UC emission based on triplet energy migration (TEM), even in air. A high UC quantum yield of 3.1% is observed for this TEM-UC system, expanding the scope of molecular sensitizers for NIR-to-vis UC.

Photon upconversion (UC) is a process that produces higher energy photons with respect to the incident light. Particularly, near-infrared (NIR)-to-visible (vis) UC has wide variety of applications ranging from solar energy conversion to biotechnology. Integrating NIR-to-vis UC materials into single-junction photovoltaic devices has potential to overcome the Shockley–Queisser limit, and may enhance the efficiency of perovskite solar cells, whose absorption is currently limited to visible light (<800 nm).[1] The high permeability of NIR light in living systems is also advantageous for biological applications, including bioimaging and photodynamic therapy.[2]

Among the existing UC mechanisms, triplet–triplet annihilation (TTA)-based UC has attracted much attention for its occurrence with low-intensity and non-coherent incident light.[3] Figure 1a shows a typical scheme for TTA-based UC, in which a molecular sensitizer (triplet donor)–emitter (triplet acceptor) pair shares roles. A triplet excited state (T_1) of the donor is formed via intersystem crossing (ISC) from the singlet excited state (S_1) of the donor. Donor-to-acceptor (D–A) triplet–triplet energy transfer (TTET) populates the T_1 state of acceptor, and TTA between two acceptor triplets produces a higher energy acceptor S_1 state that consequently emits upconverted delayed fluorescence.

Despite many efforts, implementation of NIR-to-vis TTA-UC remains challenging.[3b,c,h,4,5] The longest excitation wavelength for TTA-UC based on molecular sensitizers was 856 nm; however, this system showed a small anti-Stokes shift of 0.35 eV.[4] The difficulty stems from the donor. The energy loss during ISC, typically hundreds of meV, is considerable in the NIR region. Further, this energy loss restricts us to use acceptors with low T_1 energy level, which made the TTA process of producing S_1 with visible energy endothermic and resulted in low UC quantum

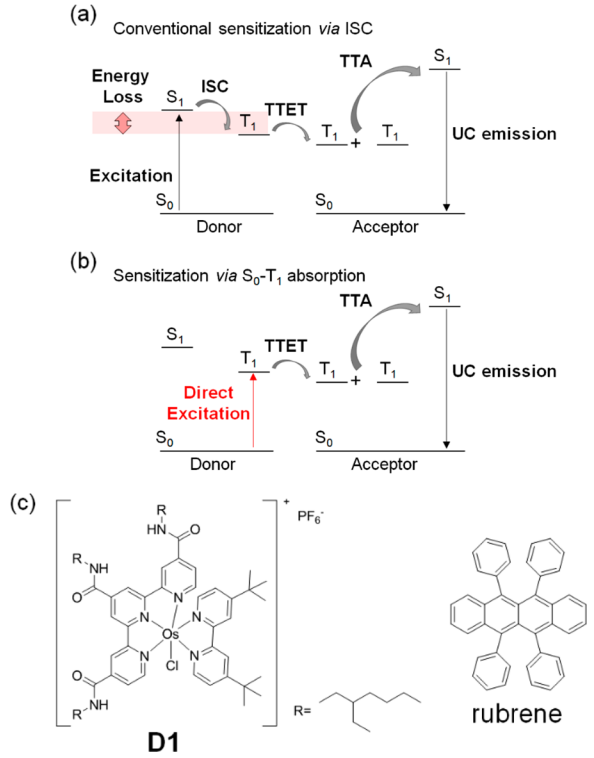

Figure 1. (a) Common TTA-based UC mechanism via donor ISC that involves energy loss. A triplet state T_1 of donor, formed by ISC from the photoexcited S_1 state, experiences TTET to an acceptor T_1. Two acceptor T_1's annihilate to form acceptor S_1 and S_0, and the former consequently produces upconverted delayed fluorescence. (b) TTA-based UC utilizing S_0–T_1 absorption of donor. The absence of energy loss due to ISC allows the large anti-Stokes shift from NIR to visible. (c) Molecular structures of donor (sensitizer) **D1** and acceptor (emitter) rubrene.

Received: May 6, 2016
Published: June 28, 2016

DOI: 10.1021/jacs.6b04692
J. Am. Chem. Soc. 2016, 138, 8702–8705

yield.[4] While there have been some recent advances using inorganic sensitizers,[3d,6] it is highly desired to develop molecular sensitizers that can minimize the dissipative energy by finely controlling the structure and energy levels on the molecular level.

Here, we report a solution for overcoming the energy loss issue in NIR-to-vis UC. This is based on eliminating the ISC process by employing a molecular sensitizer with direct S_0-T_1 absorption (Figure 1b). Although in general direct population of the T_1 state from the ground S_0 state is spin-forbidden, some metal complexes have sufficiently large absorption coefficient ($\varepsilon > 1000$) due to the strong spin−orbit coupling.[7] It has been reported that the properly designed osmium complexes show strong S_0-T_1 absorption in the NIR region, which can be utilized to harvest NIR light in dye-sensitized solar cells.[7b,c] In this work, we synthesized a new lipophilic Os complex (**D1**) soluble in organic media (Figure 1c). While the previously reported Os complexes have carboxylate groups and show solubility in water, we introduced branched alkyl chains to **D1** so that it becomes miscible with the aggregates of non-polar acceptor, rubrene. By sensitizing the rubrene triplet with **D1**, the incident NIR light beyond 900 nm (λ = 938 nm) is successfully upconverted to the visible light (λ = 570 nm) in solution. This is the first example of upconverting over 900 nm photons with a molecular sensitizer, and a remarkable anti-Stokes shift of 0.86 eV that goes beyond the previous NIR-to-vis system (0.35 eV)[4] was obtained thanks to the elimination of energy loss associated with ISC. Moreover, the efficiency of TTET process was enhanced by dispersing **D1** in the rubrene nanoassemblies. Integrating this D−A nanohybrid in an oxygen-barrier polymer, poly(vinyl alcohol) (PVA), resulted in a notably high UC quantum yield of 3.1% for NIR-to-vis TTA-UC in air.

The Os complex **D1** was synthesized and fully characterized (Scheme S1, Supporting Information (SI)). As shown in Figure 2a, a dichloromethane (DCM) solution of **D1** exhibited a singlet−triplet MLCT absorption band at 888 nm (ε = 3200) with tails extending over around 950 nm, similar to the analogous compound.[7c] Excitation of this MLCT band produced a triplet emission at ca. 1000 nm (Figure 2a).[7c] The absence of ISC process allows the small Stokes shift between the S_0-T_1 absorption and the T_1-S_0 emission.[7c,d] This is in stark contrast with the common phosphorescence process, which shows the large Stokes shift originating from the energy loss associated with the ISC. A weak emission at 1280 nm originated from singlet oxygen was observed by exciting an oxygen-bubbled **D1** solution with 890 nm NIR light, supporting the formation of **D1** triplet under NIR excitation (Figure S1, SI).

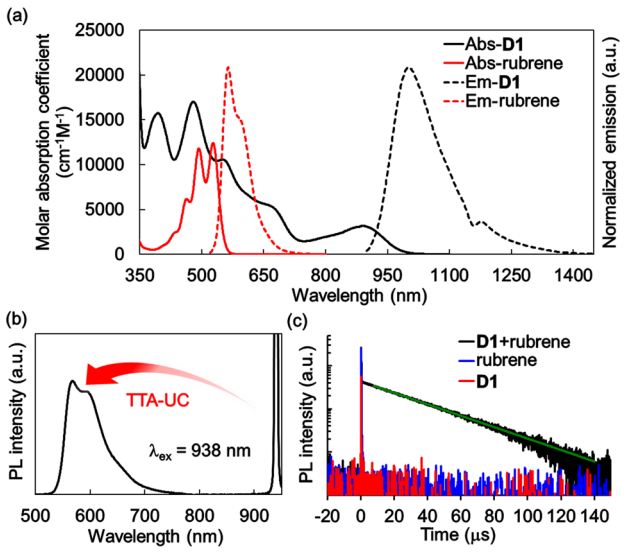

Figure 2. (a) Absorption and emission spectra of **D1** (0.1 mM, λ_{ex} = 820 nm) and rubrene (0.1 mM, λ_{ex} = 490 nm) in DCM. (b) Upconverted emission spectrum of the **D1**−rubrene pair in deaerated DCM ([**D1**] = 0.1 mM, [rubrene] = 5 mM, λ_{ex} = 938 nm, 780 nm short pass filter). (c) Time-resolved upconverted emission at 570 nm of **D1**−rubrene pair, rubrene and **D1** in deaerated DCM ([**D1**] = 0.1 mM, [rubrene] = 5 mM, λ_{ex} = 938 nm). The green fitting curve was obtained by considering the known relationship of $I_{UC}(t) \propto \exp(-2t/\tau_T)$, where τ_T is acceptor triplet lifetime.

Interestingly, under excitation at 938 nm (1.32 eV), a mixed solution of **D1** and rubrene in deaerated DCM clearly displayed an upconverted emission at 570 nm (2.18 eV) with a large anti-Stokes shift of 0.86 eV (Figure 2b). This large energy gain could be achieved by the ISC-free S_0-T_1 direct excitation.

The TTA-based UC mechanism was confirmed by the lifetime and excitation intensity dependence of the upconverted emission. The UC emission at 570 nm showed a microsecond-scale decay profile, which is ascribed to the mechanism based on long-lived triplet species (Figure 2c). Such a long decay was absent in single-component solutions of **D1** or rubrene. A triplet lifetime of acceptor rubrene (τ_T) was estimated as 66 μs by tail fitting based on the known relationship $I_{UC}(t) \propto \exp(-2t/\tau_T)$.[8] In this time domain, the annihilation efficiency becomes negligible compared with the spontaneous decay of the triplet, and thus the τ_T value can be simply estimated. The UC emission intensity from the **D1**−rubrene mixed solution was plotted as a function of excitation intensity (Figure S2, SI). A slope of 2.0 was observed in the double-logarithmic plot, which is consistent with the quadratic dependence of TTA process.

We then quantified the TTA-UC quantum yield of the **D1**−rubrene pair in deaerated DCM by using Nile red as a reference (see SI for detail). Note that the quantum yield is generally defined as the ratio of emitted photon numbers to absorbed photon numbers, and thus the theoretical maximum of the TTA-UC quantum yield (Φ_{UC}) is 50%. Meanwhile, in many reports this value is multiplied by 2 to set the maximum conversion efficiency at 100%. To avoid the confusion between these different definitions, the UC quantum yield is written as Φ_{UC}' (= $2\Phi_{UC}$) when the maximum efficiency is standardized to be 100%. With increasing the excitation intensity, the Φ_{UC}' value increased to 0.0047% at I_{ex} = 198 W cm^{-2}, but it did not reach saturation in the examined range (Figure S3, SI).

To figure out the reason for such low UC efficiency, we measured phosphorescence decays of **D1** with and without rubrene in deaerated DCM. As a result, **D1** in the absence of rubrene showed a triplet lifetime of 12 ns, while almost no difference was observed between the two decays (Figure S4, SI). This result indicates that the TTET from **D1** to rubrene hardly occur due to the short lifetime of **D1** triplet. We further increased [rubrene] to 10 mM by using chloroform as a better solvent, but it did not enhance the Φ_{UC}' value (0.0014% at I_{ex} = 212 W cm^{-2}). The low UC quantum yield, originating from the low **D1**−rubrene TTET efficiency, should be due to the short triplet lifetime of **D1**, not [rubrene]. Thus, improvement of the TTET efficiency is crucial to boost the UC quantum yield.

We found that the key to solve this issue is to take advantage of the triplet energy migration (TEM)-based UC in chromophore assemblies,[3n−t] instead of the classical molecular diffusion-based UC in solution. In TEM-UC configuration, suitable arrangement of donor molecules in the vicinity of densely pre-organized

DOI: 10.1021/jacs.6b04692
J. Am. Chem. Soc. 2016, 138, 8702−8705

acceptor assemblies allows efficient D−A Dexter energy transfer even with the short donor triplet lifetime.[3t]

We prepared **D1**-doped rubrene nanoparticles (NPs) by the reprecipitation method.[3r,t,9] A 5 mL THF solution containing **D1** (0.02 mM) and rubrene (5 mM) was rapidly injected into 25 mL of sodium dodecyl sulfate (SDS) aqueous solution (10 mM), and the formed solid particles were collected by centrifugation (see SI for more details). Absorption measurements after dissolving the precipitates in DCM showed that the initial concentration ratio in THF ([**D1**]:[rubrene] = 1:250) was almost maintained in the NPs (**D1**:rubrene = 1:270). Dynamic light scattering (DLS) measurements of **D1**−rubrene particles showed an average particle size of 237 nm (Figure 3a). Scanning electron microscopy (SEM) showed spherical NP structures with an average diameter of 220 nm (Figure 3b), which is in good agreement with the DLS result. The ζ-potential of the **D1**-doped rubrene NPs was determined as −16 mV, indicating the surface of NPs is covered with SDS. The X-ray powder diffraction (XRPD) pattern of the **D1**-doped rubrene NPs did not show any sharp peaks, indicating the amorphous structure (Figure S5, SI).

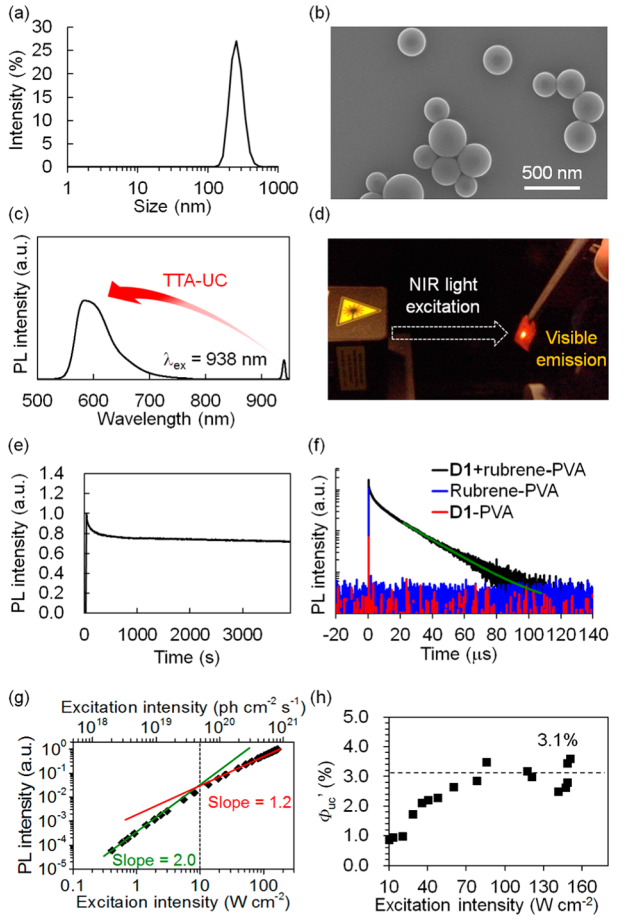

Figure 3. (a) DLS profile of the **D1**-doped rubrene NPs dispersed in water. (b) SEM image of the **D1**-doped rubrene NPs. (c) In-air upconverted emission spectrum of the **D1**-doped rubrene NPs dispersed in PVA film (λ_{ex} = 938 nm, 780 nm short pass filter). (d) Photograph of upconverted yellow emission of **D1**−rubrene in PVA film in air under 938 nm NIR excitation. (e) Time dependence of upconverted emission intensity at 580 nm of **D1**−rubrene in PVA film in air (λ_{ex} = 938 nm, laser intensity =170 W cm^{-2}). (f) Time-resolved upconverted emission at 580 nm of the **D1**−rubrene pair, rubrene and **D1** in PVA film (λ_{ex} = 938 nm). The green fitting curve was obtained by considering the relationship of $I_{UC}(t) \propto \exp(-2t/\tau_T)$, where τ_T is acceptor triplet lifetime. (g) Double-logarithmic plots of the UC emission intensity at 580 nm of **D1**−rubrene in PVA film as a function of excitation intensity of the 938 nm laser. The solid green and red lines are fitting results with slopes of 2.0 and 1.2 in the low- and high-intensity regimes, respectively. (h) Absolute UC quantum yield Φ_{UC}' of **D1**−rubrene in PVA film as a function of excitation intensity of the 730 nm laser.

Even in air, the solid film showed a stable UC emission around 580 nm under excitation at 938 nm (Figure 3c). The yellow UC emission was clearly observed by the naked eye (Figure 3d). This in-air UC emission showed excellent photochemical stability, as confirmed by the good maintenance of UC emission intensity after continuous excitation over 4000 s (Figure 3e). The initial dip and following slow decrease are probably caused by the quenching of excited triplets by remaining oxygen molecules in the PVA film and slowly intruding oxygen molecules into the film from air, respectively. The UC emission at 580 nm showed a microsecond-scale decay, and a long triplet lifetime τ_T = 38 μs was observed in the solid film geometry (Figure 3f).

In contrast to the solution system, a slope change from 2 to 1 was clearly observed in double-logarithmic plots of the UC emission intensity of the solid film against excitation intensity (Figure 3g). Generally, the excitation intensity dependence of UC emission intensity changes from quadratic to linear above a threshold excitation intensity (I_{th}).[11] Above I_{th}, TTA becomes the main deactivation channel for the acceptor triplet, and consequently the UC quantum yield shows saturation. The observed slope change implies that the TTA process of the solid system was more efficient compared with the solution system.

We actually observed much higher UC quantum yield for the solid film system in air than those observed for the deaerated solution. The absolute method with integrating sphere was used to measure Φ_{UC}' due to the scattering of the solid sample.[3q] Because of the insufficient sensitivity of the detector at 938 nm, we used a 730 nm laser as the excitation source. We observed the similar I_{th} values in the excitation intensity dependence of UC emission intensity under excitations at 730 nm (17 W cm^{-2}, 6.2 × 10^{19} photons cm^{-2} s^{-1}, Figure S6, SI) and 938 nm (10 W cm^{-2}, 4.7 × 10^{19} photons cm^{-2} s^{-1}, Figure 3g). No UC emission was observed from a single component of **D1** or rubrene in PVA under the 730 nm excitation. Significantly, a high Φ_{UC}' value of 3.1% was observed for the solid film (Figure 3h).

To understand the much improved Φ_{UC}' value, we examined the phosphorescence lifetime of **D1**. For this, we need a standard sample without rubrene for comparison. The peak position of only **D1** in PVA film showed a red shift (1040 nm) compared with the **D1**−rubrene nanohybrid in PVA (975 nm), probably owing to the aggregation of **D1** in PVA (Figure S7, SI). Aggregation of **D1** molecules in PVA was obvious even by eye. In contrast, the **D1** molecules could be nicely dispersed in poly(methyl methacrylate) (PMMA), and the emission wavelength of **D1** in PMMA was almost identical to that of **D1**−rubrene in PVA, so we employed this sample for comparison (Figure S7, SI). The shorter phosphorescence lifetime for **D1**−rubrene in PVA than **D1** in PMMA suggests the effective TTET from **D1** to rubrene (Figure S8, SI). This Dexter energy-transfer process in the solid film was attained by means of the close

DOI: 10.1021/jacs.6b04692
J. Am. Chem. Soc. 2016, 138, 8702−8705

contact between **D1** and rubrene in the co-assembled TEM-UC system. It has been reported that sensitizer molecules have strong tendency to aggregate in emitter crystals.[12] In contrast, the current amorphous structure of rubrene NPs allows to host sensitizer **D1** molecules doped without aggregation, which was confirmed by the absence of prominent shift in **D1** photoluminescence peak (Figure 2a and Figure S7, SI) and by the high UC quantum yield of 3.1%.

In conclusion, we demonstrate that the molecular sensitizer with spin-forbidden yet strong S_0-T_1 absorption reduces the energy loss during triplet sensitization and enables upconverting NIR light beyond 900 nm to visible light. While the triplet lifetime of this kind of sensitizer is short, implementing the TEM-UC approach allows efficient Dexter energy transfer to the neighboring acceptors, leading to solid films with high UC quantum yield and good in-air photochemical stability. This work underlines the importance of the TEM-UC concept and stimulates the exploration of new S_0-T_1 absorption-type molecular sensitizers toward highly efficient NIR-to-vis molecular upconverters, which would find a number of applications in many disciplines.

■ ASSOCIATED CONTENT

Supporting Information

The Supporting Information is available free of charge on the ACS Publications website at DOI: 10.1021/jacs.6b04692.

Experimental details, emission spectra, XRPD patterns, excitation dependence of UC emission intensity, UC quantum yield, and emission lifetime (PDF)

■ AUTHOR INFORMATION

Corresponding Authors

*yanai@mail.cstm.kyushu-u.ac.jp

*n-kimi@mail.cstm.kyushu-u.ac.jp

Author Contributions

§S.A. and Y.S. contributed equally.

Notes

The authors declare no competing financial interest.

■ ACKNOWLEDGMENTS

This work was partially supported by a Grant-in-Aid for Scientific Research (S) (25220805), a Grant-in-Aid for Scientific Research on Innovative Area (16H00844) from the Ministry of Education, Culture Sports, Science and Technology of Japan, the JSPS-NSF International Collaborations in Chemistry (ICC) program, and the Asahi Glass Foundation. S.A. acknowledges the Research Fellowship from the Japan Society for the Promotion of Science for Young Scientists.

■ REFERENCES

(1) (a) Shockley, W.; Queisser, H. J. *J. Appl. Phys.* **1961**, *32*, 510. (b) de Wild, J.; Meijerink, A.; Rath, J. K.; van Sark, W. G. J. H. M.; Schropp, R. E. I. *Energy Environ. Sci.* **2011**, *4*, 4835. (c) Schulze, T. F.; Schmidt, T. W. *Energy Environ. Sci.* **2015**, *8*, 103.

(2) Zhou, J.; Liu, Q.; Feng, W.; Sun, Y.; Li, F. *Chem. Rev.* **2015**, *115*, 395.

(3) (a) Baluschev, S.; Yakutkin, V.; Miteva, T.; Avlasevich, Y.; Chernov, S.; Aleshchenkov, S.; Nelles, G.; Cheprakov, A.; Yasuda, A.; Müllen, K.; Wegner, G. *Angew. Chem., Int. Ed.* **2007**, *46*, 7693. (b) Yakutkin, V.; Aleshchenkov, S.; Chernov, S.; Miteva, T.; Nelles, G.; Cheprakov, A.; Baluschev, S. *Chem. - Eur. J.* **2008**, *14*, 9846. (c) Singh-Rachford, T. N.; Nayak, A.; Muro-Small, M. L.; Goeb, S.; Therien, M. J.; Castellano, F. N. *J. Am. Chem. Soc.* **2010**, *132*, 14203. (d) Mongin, C.; Garakyaraghi, S.; Razgoniaeva, N.; Zamkov, M.; Castellano, F. N. *Science* **2016**, *351*, 369. (e) Liu, Q.; Yin, B.; Yang, T.; Yang, Y.; Shen, Z.; Yao, P.; Li, F. *J. Am. Chem. Soc.* **2013**, *135*, 5029. (f) Mahmood, Z.; Zhao, J. *J. Org. Chem.* **2016**, *81*, 587. (g) Vadrucci, R.; Weder, C.; Simon, Y. C. *Mater. Horiz.* **2015**, *2*, 120. (h) Fückel, B.; Roberts, D. A.; Cheng, Y. Y.; Clady, R. G. C. R.; Piper, R. B.; Ekins-Daukes, N. J.; Crossley, M. J.; Schmidt, T. W. *J. Phys. Chem. Lett.* **2011**, *2*, 966. (i) Nattestad, A.; Cheng, Y. Y.; MacQueen, R. W.; Schulze, T. F.; Thompson, F. W.; Mozer, A. J.; Fückel, B.; Khoury, T.; Crossley, M. J.; Lips, K.; Wallace, G. G.; Schmidt, T. W. *J. Phys. Chem. Lett.* **2013**, *4*, 2073. (j) Kim, J.-H.; Kim, J.-H. *J. Am. Chem. Soc.* **2012**, *134*, 17478. (k) Gray, V.; Dzebo, D.; Lundin, A.; Alborzpour, J.; Abrahamsson, M.; Albinsson, B.; Moth-Poulsen, K. *J. Mater. Chem. C* **2015**, *3*, 11111. (l) Hoseinkhani, S.; Tubino, R.; Meinardi, F.; Monguzzi, A. *Phys. Chem. Chem. Phys.* **2015**, *17*, 4020. (m) Monguzzi, A.; Mauri, M.; Bianchi, A.; Dibbanti, M. K.; Simonutti, R.; Meinardi, F. *J. Phys. Chem. C* **2016**, *120*, 2609. (n) Baluschev, S.; Yakutkin, V.; Wegner, G.; Minch, B.; Miteva, T.; Nelles, G.; Yasuda, A. *J. Appl. Phys.* **2007**, *101*, 023101. (o) Vadrucci, R.; Weder, C.; Simon, Y. C. *J. Mater. Chem. C* **2014**, *2*, 2837. (p) Duan, P.; Yanai, N.; Kimizuka, N. *J. Am. Chem. Soc.* **2013**, *135*, 19056. (q) Duan, P.; Yanai, N.; Nagatomi, H.; Kimizuka, N. *J. Am. Chem. Soc.* **2015**, *137*, 1887. (r) Ogawa, T.; Yanai, N.; Monguzzi, A.; Kimizuka, N. *Sci. Rep.* **2015**, *5*, 10882. (s) Mahato, P.; Monguzzi, A.; Yanai, N.; Yamada, T.; Kimizuka, N. *Nat. Mater.* **2015**, *14*, 924. (t) Yanai, N.; Kimizuka, N. *Chem. Commun.* **2016**, *52*, 5354.

(4) Amemori, S.; Yanai, N.; Kimizuka, N. *Phys. Chem. Chem. Phys.* **2015**, *17*, 22557.

(5) Yakutkin, V.; Filatov, M. A.; Ilieva, I. Z.; Landfester, K.; Miteva, T.; Baluschev, S. *Photochem. Photobiol. Sci.* **2015**, DOI: 10.1039/c5pp00212e.

(6) (a) Huang, Z.; Li, X.; Mahboub, M.; Hanson, K. M.; Nichols, V. M.; Le, H.; Tang, M. L.; Bardeen, C. J. *Nano Lett.* **2015**, *15*, 5552. (b) Wu, M.; Congreve, D. N.; Wilson, M. W. B.; Jean, J.; Geva, N.; Welborn, M.; Voorhis, T. V.; Bulovic, V.; Bawendi, M. G.; Baldo, M. A. *Nat. Photonics* **2016**, *10*, 31. (c) Huang, Z.; Simpson, D. E.; Mahboub, M.; Li, X.; Tang, M. L. *Chem. Sci.* **2016**, *7*, 4101. (d) Okumura, K.; Mase, K.; Yanai, N.; Kimizuka, N. *Chem. - Eur. J.* **2016**, *22*, 7721.

(7) (a) Lamansky, S.; Djurovich, P.; Murphy, D.; Abdel-Razzaq, F.; Lee, H. E.; Adachi, C.; Burrows, P. E.; Forrest, S. R.; Thompson, M. E. *J. Am. Chem. Soc.* **2001**, *123*, 4304. (b) Altobello, S.; Argazzi, R.; Caramori, S.; Contado, C.; Da Fre, S.; Rubino, P.; Chone, C.; Larramona, G.; Bignozzi, C. A. *J. Am. Chem. Soc.* **2005**, *127*, 15342. (c) Kinoshita, T.; Fujisawa, J.; Nakazaki, J.; Uchida, S.; Kubo, T.; Segawa, H. *J. Phys. Chem. Lett.* **2012**, *3*, 394. (d) Kinoshita, T.; Dy, J. T.; Uchida, S.; Kubo, T.; Segawa, H. *Nat. Photonics* **2013**, *7*, 535. (e) Zhang, X.; Canton, S. E.; Smolentsev, G.; Wallentin, C.-J.; Liu, Y.; Kong, Q.; Attenkofer, K.; Stickrath, A. B.; Mara, M. W.; Chen, L. X.; Wärnmark, K.; Sundström, V. *J. Am. Chem. Soc.* **2014**, *136*, 8804.

(8) (a) Pope, M.; Swenberg, C. E. *Electronic Processes in Organic Crystals and Polymers*; Oxford University Press: New York, 1999. (b) Monguzzi, A.; Frigoli, M.; Larpent, C.; Tubino, R.; Meinardi, F. *Adv. Funct. Mater.* **2012**, *22*, 139.

(9) (a) Pecher, J.; Mecking, S. *Chem. Rev.* **2010**, *110*, 6260. (b) Thévenaz, D. C.; Lee, S. H.; Guignard, F.; Balog, S.; Lattuada, M.; Weder, C.; Simon, Y. C. *Macromol. Rapid Commun.* **2016**, *37*, 826.

(10) (a) Wohnhaas, C.; Friedemann, K.; Busko, D.; Landfester, K.; Baluschev, S.; Crespy, D.; Turshatov, A. *ACS Macro Lett.* **2013**, *2*, 446. (b) Svagan, A. J.; Busko, D.; Avlasevich, Y.; Glasser, G.; Baluschev, S.; Landfester, K. *ACS Nano* **2014**, *8*, 8198.

(11) (a) Monguzzi, A.; Mezyk, J.; Scotognella, F.; Tubino, R.; Meinardi, F. *Phys. Rev. B: Condens. Matter Mater. Phys.* **2008**, *78*, 195112. (b) Cheng, Y. Y.; Fückel, B.; Khoury, T.; Clady, R. G. C. R.; Tayebjee, M. J. Y.; Ekins-Daukes, N. J.; Crossley, M. J.; Schmidt, T. W. *J. Phys. Chem. Lett.* **2010**, *1*, 1795. (c) Haefele, A.; Blumhoff, J.; Khnayzer, R. S.; Castellano, F. N. *J. Phys. Chem. Lett.* **2012**, *3*, 299.

(12) Monguzzi, A.; Tubino, R.; Hoseinkhani, S.; Campione, M.; Meinardi, F. *Phys. Chem. Chem. Phys.* **2012**, *14*, 4322.